



# Electrochemical hydrogenation and desulfurization of thiophenic compounds over MoS<sub>2</sub> electrocatalyst using a different membrane-electrode assembly

Foad Mehri<sup>a, b</sup>, Soosan Rowshanzamir<sup>a, b, c</sup>

<sup>a</sup> School of Chemical Engineering, Iran University of Science and Technology, Tehran, Iran.

<sup>b</sup> Fuel Cell Laboratory, Green Research Centre, Iran University of Science and Technology, Tehran, Iran.

<sup>c</sup> Center of Excellence for Membrane Science and Technology, Iran University of Science and Technology, Tehran, Iran.

## ARTICLE INFO

### Article history:

Received 5 May 2019

Received in revised form

16 July 2019

Accepted 7 August 2019

### Keywords:

Hydrogenation

Desulfurization

Thiophenic

MoS<sub>2</sub> electrocatalyst

Membrane-electrode assembly

## ABSTRACT

The desulfurization-hydrogenation of thiophene and benzothiophene in hexadecane as a model diesel fuel was studied through a divided cell with the incorporation of a membrane electrode assembly (MEA) under different current density at a constant charge. The reduction of the thiophenic compounds was investigated using a prepared MoS<sub>2</sub> nano-electrocatalyst, Nafion (commercial proton exchange membrane), and synthesized sulfonated poly ether ether ketone (SPEEK). Field emission scanning electron microscopy (FESEM) and X-ray diffraction (XRD) were used to characterize the MoS<sub>2</sub> electrocatalyst, which confirmed the formation of 23-25 nm ball-like nano-threads of MoS<sub>2</sub>. Also, the electrocatalyst and/or MEA was electrochemically analyzed by cyclic voltammetry (CV), linear sweep voltammetry (LSV), and electrochemical impedance spectroscopy (EIS). The gas chromatography-mass spectroscopy (GC-MS) analysis of the reactants and products revealed the direct desulfurization on the thiophene reduction process and the desulfurization along with the desulfurization pathway on the benzothiophene reduction experiment. A maximum desulfurization efficiency of 79.6% at 20 mA cm<sup>-2</sup> and 51.5% at 30 mA cm<sup>-2</sup> under the constant charge of 300 C was obtained for thiophene using the MoS<sub>2</sub>-Nafion and MoS<sub>2</sub>-SPEEK system, respectively. Moreover, a maximum hydrogenation and desulfurization efficiency of 28% and 59.1% occurred at 50 mA cm<sup>-2</sup> and 70 mA cm<sup>-2</sup>, respectively, for the benzothiophene-Nafion system under the constant charge of 400 C. The distribution of the products affirmed that the desulfurization reaction contributed more at a higher current density against the hydrogenation process at a lower current density.

## 1. Introduction

Typical organic sulfur compounds found in oil include thiophene, benzothiophene, dibenzothiophene, benzonaphthothiophene, mercaptans, sulfides, etc. [1]. Sulfur oxides (SOx) are a major source of air pollution and environmental problems that is mainly caused by the combustion of fossil fuels. In recent years, strict regulations have been legislated to reduce the sulfur content in transportation fuels [2,3]. Thus, great efforts have been made to decrease the sulfur content in fossil fuels [4-6].

Currently, hydrodesulfurization (HDS) is the most commonly used desulfurization method; it is conducted under high pressure and elevated temperature, and it also requires high energy consumption and a host of processing equipment [7,8]. Regarding the limited efficiency of HDS toward the desulfurization of thiophenic compounds [9,10], several new technologies such as catalytic oxidation desulfurization [11-13], selective adsorption desulfurization [14,15], extraction desulfurization, biodesulfurization, and electrochemical desulfurization have been proposed [16,17]. Among the new desulfurization technologies,

\*Corresponding author. Tel: +98 2177491223

E-mail address: rowshanzamir@iust.ac.ir

DOI: 10.22104/aet.2019.3647.1178

electrochemical desulfurization is a promising technique that is environmentally friendly and low cost [18]. It allows for the controlling of the distribution of products by adjusting the applied potential or by controlling the overall conversion rate by setting the applied current. Also, the experiments can be carried out at an ambient temperature and pressure; promising results have been reported using this technology [19]. Electrochemical desulfurization (ECDS) technology can be carried out in a divided cell to bypass the need for mixing the aqueous electrolyte with the organic fuel, which is a necessary step when an undivided cell is used [20]. In these types of cells, the cathode and anode are separated from each other by an ion-exchange membrane. Typically, water is oxidized to oxygen, a proton, and an electron. The protons ( $H^+$ ) can migrate through a proton exchange membrane (PEM) such as commercial Nafion and combine with an electron to reduce the organics in the catholyte. Despite numerous researches about the reduction or hydrogenation of organics using an electrochemical membrane reactor [21-23], a few studies have been devoted to the fuel desulfurization of refractory sulfurs (i.e., thiophenic compounds). Baez *et al.* [24] investigated the removal of sulfur from a hydrocarbon feedstock containing thiophene by applying a constant current. They simultaneously used a divided cell with palladium metal as a membrane and a working electrode so that separating the electrolyte from the desulfurized products was not required. The results illustrated the removal of 35% thiophene from the fuel after 24 h. Greaney *et al.* [25] used a separated cell by a permeable ion-membrane for electrochemical desulfurization of hard sulfur compounds. In their study, heated and pressurized (204 °C and 200 psig) hydrocarbon feedstock entered into the cathode chamber under hydrogen gas, and sulfur compounds were reduced to hydrogen sulfide. Then, the hydrogen sulfide was sent back to the anode chamber to be oxidized and generate protons. Via this method, a conversion higher than 90% was obtained for dibenzothiophene for 164 h. Camacho *et al.* [26] performed the electrochemical reduction of thiophenic compounds by passing active hydrogen through a palladium membrane, and relatively high conversions (25–50%) were achieved for the reactions performed under mild conditions (25 °C and 1.0 atm) at 1.92 mA cm<sup>-2</sup>.

In spite of using a proton exchange membrane with an acceptable ionic conductivity in an electrochemical membrane reactor toward desulfurization, incorporating a cathode and an efficient electrocatalyst for the reduction of thiophenic compounds are the other main concerns of this type of electrochemical cell. Nafion, as the most conventional PEM, has been frequently used in electrochemical divided cells [27,28], and other less expensive alternatives to PEM can also be used [29-33]. Platinum is the most active electrode among the precious metals for the desulfurization of thiophenic compounds,

but it suffers from high cost and has a tendency to be toxic and/or passivation occurs during the experiment [34,35]. Also, its low overpotential for a hydrogen evolution reaction (HER) as a side reaction during reduction decreases the current efficiency [36]. So, finding an appropriate electrocatalyst with high activity toward desulfurization and a high overpotential toward the hydrogen evolution reaction is essential to overcome the present challenges. In this context, few electrocatalysts have been used for desulfurization individually and/or integrated with a PEM. For example, Shu *et al.* [37] desulfurized diesel fuel by sodium borohydride in situ generated via sodium metaborate electroreduction in a divided cell. Under the optimal conditions, a desulfurization efficiency of 93% was obtained for 3-methyl benzothiophene (3-MBT) and dibenzothiophene (DBT) in *n*-decane as the model diesel fuel. Huang *et al.* [38] performed the electrochemical reduction desulfurization of thiophene and benzyl mercaptan on C/Nafion electrodes at -0.35 V at 50 °C for over 2 h, and the conversion of 70% and 15% were obtained, respectively. In selecting an electrocatalyst for the electroreduction of refractory sulfurs, the use of HDS catalysts can be useful, since the hydrogen adsorption on this catalyst under high temperature and pressure is similar to that which occurs on electrocatalysts under specified potential or current. In this regard, the transition metal sulfides are an interesting group of catalysts used in the hydrodesulfurization process [39]. Their unique structure has led to their use in various processes, including catalytic hydrodesulfurization of petroleum [40,41], electrohydrogenation [42], lithium-ion batteries [43], supercapacitors [44], and lubricants [45]. Molybdenum disulfide ( $MoS_2$ ) is one of the catalysts used in the desulfurization process; its use in the HDS process is very common and has shown good performance owing to its high chemical stability, low cost, and excellent electrocatalytic performance [46]. Also, molybdenum disulfide as an efficient catalyst for the desulfurization of refractory sulfur and has been investigated extensively [40,47].  $MoS_2$  has a stacked layer structure in which each layer of molybdenum is sandwiched between two sulfide layers. The van der Waals forces between the layers provide a degree of freedom for them to move back and forth. This property is of importance in its catalytic performance [48]. The structure of the nano-sized bulk molybdenum sulfide is important because it is linked to the catalytic performance. The activity of  $MoS_2$  in both the hydroprocessing and hydrotreating reactions is dependent upon the morphology of the catalyst, and several studies have reported on the structure-activity relationships for  $MoS_2$  catalysts [48]. In this research,  $MoS_2$  as a new desulfurization electrocatalyst with a higher hydrogen evolution overpotential than that of platinum was synthesized, characterized, and investigated toward the desulfurization of thiophene and benzothiophene in a diesel model fuel (hexadecane) using

an electrochemical membrane reactor. Two different proton exchange membranes of Nafion and synthesized sulfonated poly ether ether ketone was examined in the electroreductive desulfurization of the model diesel fuel under different applied constant currents. The fuel was analyzed with GC-MS to determine the desulfurization efficiency, initial feed, and final desulfurized model.

## 2. Materials and methods

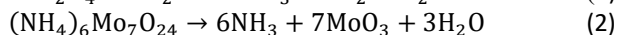
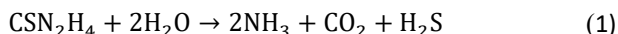
### 2.1. Chemicals

All chemicals used in this study were of analytical grade. The sulfuric acid, ethanol (C<sub>2</sub>H<sub>5</sub>OH, 99 %), acetone (C<sub>3</sub>H<sub>6</sub>O, 99 %), ammonium heptamolybdate tetrahydrate ((NH<sub>4</sub>)<sub>6</sub>Mo<sub>7</sub>O<sub>24</sub>, 99 %), thiourea (CH<sub>4</sub>N<sub>2</sub>S, 99 %), Dimethylformamide (C<sub>3</sub>H<sub>7</sub>NO, 99 %) were used as purchased (Merck company) without purification. The thiophene, T, (C<sub>4</sub>H<sub>4</sub>S, ≥99%), benzothiophene, BT, (C<sub>8</sub>H<sub>6</sub>S, ≥99%), Poly (oxy-1,4-phenyleneoxy-1,4-phenylenecarbonyl-1,4-phenylene), (PEEK), average M<sub>w</sub> ~20800, average M<sub>n</sub> ~10300 and Hexadecane (ReagentPlus®, 99%), Nafion™ 117 proton exchange membrane (thickness: 183 μm), D521 Nafion ionomer dispersion (Alcohol-based 1100 EW at 5 wt.%), and Toray Paper (TGPH-60, thickness of 190 μm) were purchased from the Fuel Cell Store. The aqueous solutions were made from deionized water. The simulated diesel fuel with a sulfur content of 2000 mg/l was prepared by dissolving T and/or BT in n-hexadecane.

### 2.2. Electrocatalyst synthesis and MEA preparation

#### 2.2.1. MoS<sub>2</sub> nanosheets synthesis

The MoS<sub>2</sub> nanosheets were prepared by a one-step hydrothermal reaction using ammonium heptamolybdate tetrahydrate and thiourea as the molybdenum and sulfur source, respectively, based on the reaction indicated in Eqs. (1) to (4). First, 1.24 g of (NH<sub>4</sub>)<sub>6</sub>Mo<sub>7</sub>O<sub>24</sub> and 2.28 g of N<sub>2</sub>H<sub>4</sub>CS were dissolved in 36 ml of deionized water under stirring for over 60 min to provide a homogeneity in the final solution. The solution was then poured into a 100 ml Teflon-lined stainless steel autoclave and heated at 220 °C for 24 h, and then it was cooled down to 25 °C. The resultant black precipitates were washed and centrifuged several times with distilled water, ethanol, and acetone. The final precipitate was dried in vacuum at 70 °C for 20 h.



#### 2.2.2. Membrane electrode assembly (MEA) preparation

The SPEEK was prepared according to the work of Sarirchi *et al.* [49]. The MEA was prepared in the following manner. First, the well-dispersed catalyst ink was made by mixing 5.0 mg of MoS<sub>2</sub> powder with 66.7 mg of a 5wt% Nafion ionomer, 0.1 mL deionized water, and 0.2 mL

dimethylformamide. Then, the prepared catalyst ink was spray-coated on 5wt% Teflon treated carbon paper with a geometric area of 5.0 cm<sup>2</sup> at the loading of 0.5 mg cm<sup>-2</sup> and dried in air at ambient temperature. Finally, the catalyst coated carbon paper was hot-pressed on one side of the pretreated Nafion and/or SPEEK membrane at 0.7 MPa for 2.0 min at 120 °C and 0.9 MPa for 2.0 min at 130 °C, respectively.

### 2.3. Physical and chemical analysis

The X-ray diffraction patterns of the catalysts were taken using a Siemens D5000 powder diffractometer using Cu-Kα radiation. The morphology of the samples was studied using a field emission scanning electron microscope via a Zeiss microscope under an accelerating voltage of 15.0 kV purposing. The 2θ range was from 5° to 50°, and the scanning rate was 5°min<sup>-1</sup>. The quantitative elemental analysis of the nanoparticles was done by an energy dispersive X-ray microanalyzer (EDS, TESCAN model) in the range of 300–20 kV. The analysis of the desulfurized model fuel was performed using a gas chromatography-mass spectroscopy instrument (Agilent 7890A/5975C System) equipped with an HP-5MS capillary GC column (30 m × 0.5 mm × 0.25 μm). The injector temperature was 275 °C, and the column temperature was programmed from 80 °C (4 min) to 330 °C (5 min) at 25 °C/min. The column head pressure was 7.5 psig, and helium was employed as the carrier gas. A split/splitless injection was employed. The transfer line to the MS was held at 325 °C. The injection volume was 1.0 μL, with a 20:1 split ratio. The mass spectra were measured at an ionization voltage of 70 eV with a range of 40-500 amu in an ion source temperature of 200 °C full-scan mode.

### 2.4. Electrochemical analysis

All electrochemical characterizations of the MoS<sub>2</sub> electrocatalyst were performed by the aid of electrocatalyst coated glassy carbon (2.0 mm diameter) as the working electrode, platinum as the counter electrode, and an Ag/AgCl (sat. KCl) reference electrode (SE11, Sorsorteknik Meinsberg, Germany) using a divided cell in a solution containing 2000 mg/l of T and/or BT in 1.0 M H<sub>2</sub>SO<sub>4</sub>. The CV of each electrocatalyst was taken to find the appropriate potential and its corresponding current density at which the release of hydrogen and oxygen does not occur. Furthermore, the electrochemical behavior and stability of the electrocatalysts and surface reactions involved in the related working potential range could be understood [50]. Also, linear sweep voltammetry of the electrocatalysts was conducted over a given potential range to determine the overpotential of each of the working electrodes in the reduction of the sulfur compounds toward the hydrogen evolution reaction as an undesired reaction. Galvanostatic electrochemical impedance spectroscopy (GEIS) of the electrocatalyst was performed in the range of 300 kHz down

to 10.0 mHz at the best current density toward desulfurization to identify the charge transfer resistance of the electrocatalyst associated to the desulfurization of the sulfur compounds. Finally, the electrochemical active surface area (ECSA) of the electrocatalysts was examined based on the charge of adsorption of hydrogen in the potential region of the voltammogram of the electrocatalyst before H<sub>2</sub> evolution as described by McCrum *et al.* [51]. This method is applicable for those electrocatalyst showing hydrogen adsorption or a desorption peak in their respective voltammogram [52]. Thus, the ECSA (m<sup>2</sup> mg<sup>-1</sup>) was calculated according to Eq. (5):

$$ECSA = \frac{Q_H}{210 \times l} \quad (5)$$

where  $Q_H$  (μC) is the total amount of charge concerning the voltammetric peaks for the hydrogen adsorption or desorption before the hydrogen evolution potential, 210 (μC cm<sup>-2</sup>) is the amount of charge that corresponds to the adsorption of one hydrogen atom per unit surface area of the substrate, and  $l$  (mg) is the loading value of the electrocatalyst coated on the glassy carbon electrode.

The proton conductivity of the membranes was determined using electrochemical impedance measurements using a Biologic SP-150 frequency response analyzer over a frequency range from 1 Hz to 700 kHz at an AC amplitude of 10 mV. The H<sup>+</sup> conductivity,  $\sigma$ , (S cm<sup>-1</sup>) was calculated using Eq. (6):

$$\sigma = \frac{L}{R_m \times S} \quad (6)$$

where  $L$  is the dry membrane thickness (m),  $S$  is the surface area of the membrane (m<sup>2</sup>), and  $R_m$  is the resistance of the membrane (Ω) determined from the first intercept at the Z' real axis (at high frequency) of the Nyquist plot.

### 2.5. Desulfurization experiment

All the experiments were conducted under a different constant current density (galvanostatic control) using a potentiostat/galvanostat SP150 (Bio-Logic SAS, Claix, France) at ambient temperature. A three-electrode configuration was used: platinum as the counter electrode, Ag/AgCl (sat. KCl) as the reference electrode (SE11, Sensortechnik Meinsberg, Germany), and the working electrode was MoS<sub>2</sub> coated carbon paper (diameter of 2.52 cm) integrated with a proton exchange membrane such as Nafion and/or SPEEK. As schematically depicted in Figure. 1, the reactions were carried out in duplicates in H-type glass divided cells with 20.0 mL of either anolyte containing 1.0 M H<sub>2</sub>SO<sub>4</sub> or catholyte including 2000 mg/l of T and/or BT in n-hexadecane. The catholyte and anolyte were stirred continuously with magnetic stirrers.

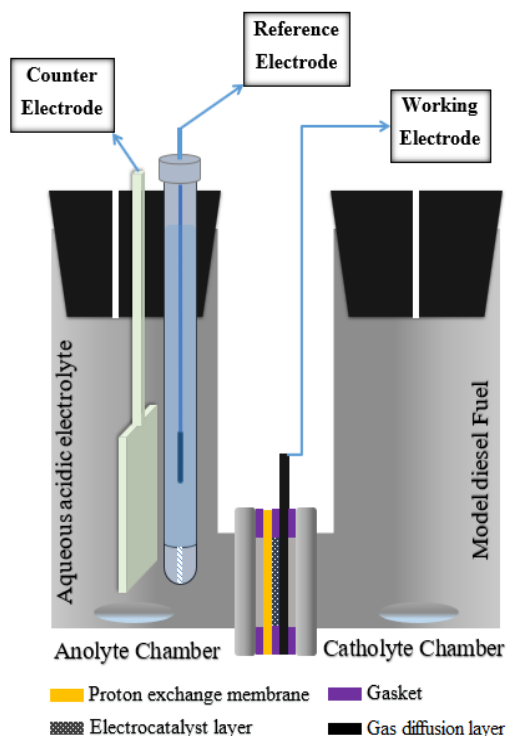


Fig. 1. Schematic of the electrochemical divided cell with MEA.

The conversion of thiophene (T) and the selectivity of the products were calculated by Eq. (7) and Eq. (8), respectively:

$$\text{Conversion (mol. \%)} = \frac{n_T^I - n_T^F}{n_T^I} \times 100 \quad (7)$$

Selectivity of products (i) =

$$\frac{\text{amount of T consumed to produce specific product (i)}}{\text{Total amount of T converted}} \times 100 = \quad (8)$$

$$\frac{n_T^{i, \text{consumed}}}{n_T^I - n_T^F}$$

Where  $n_T^I$  and  $n_T^F$  are the initial and final mole value of the thiophene and  $n_T^{i, \text{consumed}}$  is the number of mole of thiophene that is consumed based on the amount of specific detected product. During the experiment, H<sub>2</sub>S gas, as a product of desulfurization, was detected by the lead (II)-acetate. Thus, the outlet gas stream of the cell was passed through the lead acetate impregnated filter paper, which was fixed at the top of the gas-washing bottle. A light spot (positive result for H<sub>2</sub>S) formed, which turned to a dark color during the time.

## 3. Results and discussion

### 3.1. Characterizations of electrocatalyst

As can be seen in Figure 2a, the MoS<sub>2</sub> has an aggregated ball-like morphology with nano-threads. According to Figure 2b, the average size of each ball is about 500 nm with threads in the diameter range of 23-55 nm. An energy-dispersive X-ray spectrometer was also utilized to estimate the elemental composition of the electrocatalyst sample.

Figure 2c shows that Mo and S are the only elements in the sample and no other element was determined, except a negligible trace of Mo metal. Furthermore, according to the

peaks, the atomic ratio between Mo and S was about 1:1.99, which was very close to the stoichiometric MoS<sub>2</sub>.

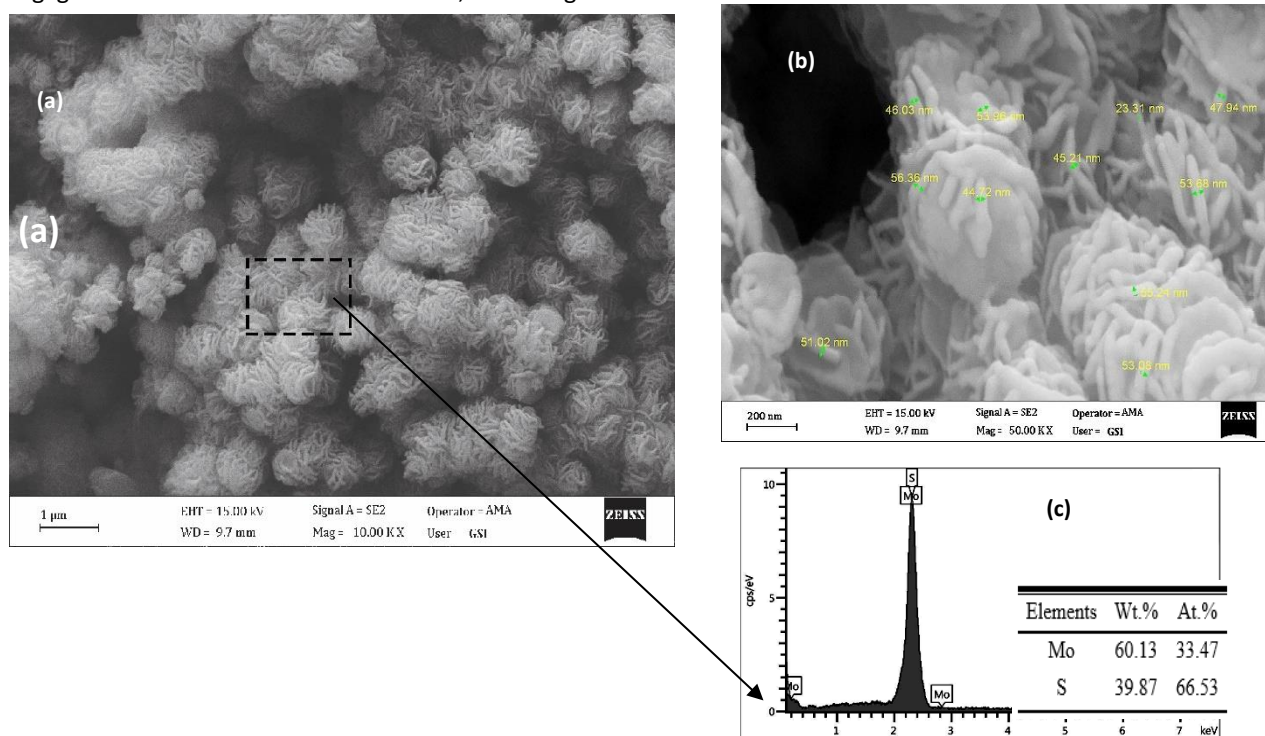


Fig. 2. (a), (b) FESEM image and (c) EDS spectrum of MoS<sub>2</sub> aggregated ball-like nano-threads.

As shown in Figure 3, the diffraction peaks at 14.0, 33.4, 34.1, 38.2 and 39.8 can be attributed to the reflections of (002), (100), (101), (103) crystal planes of hexagonal (P63/mmc space group) phase of MoS<sub>2</sub> respectively with lattice constants of  $a = b = 3.16 \text{ \AA}$  and  $c = 12.29 \text{ \AA}$ , which are consistent with the reported values (ICSD Ref. No. 01-087-2416). This result confirms that pure MoS<sub>2</sub> is obtained by the synthesis method. Also, the sharp (002) peak in the XRD pattern demonstrates the formation of crystalline MoS<sub>2</sub> with ordered stacking along the c-axis. Moreover, the crystal size of 5.7 nm obtained for the MoS<sub>2</sub> was based on the Scherrer equation.

Figure 4 shows the voltammogram of the MoS<sub>2</sub> electrocatalyst coated on the glassy carbon electrode, which is conducted in the potential range of  $-0.80 \text{ V}$  to  $1.90 \text{ V}$  in T and BT (2000 mg/l) containing  $1.0 \text{ M H}_2\text{SO}_4$ . Two distinct peaks appear on the blank electrolyte (i.e., without T and/or BT) voltammogram which is related to the oxidation of MoS<sub>2</sub> to MoO<sub>3</sub> at  $1.30 \text{ V}$  according to Eq. (9) and the adsorption of H<sup>+</sup> on the surface of MoS<sub>2</sub> at  $-0.20 \text{ V}$  according to Eq. (10).

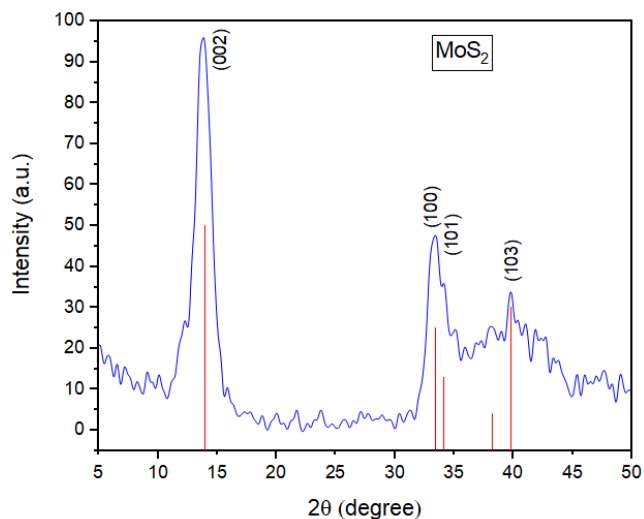
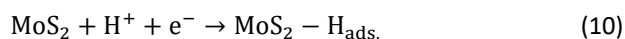
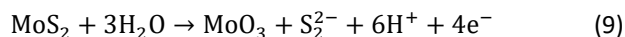
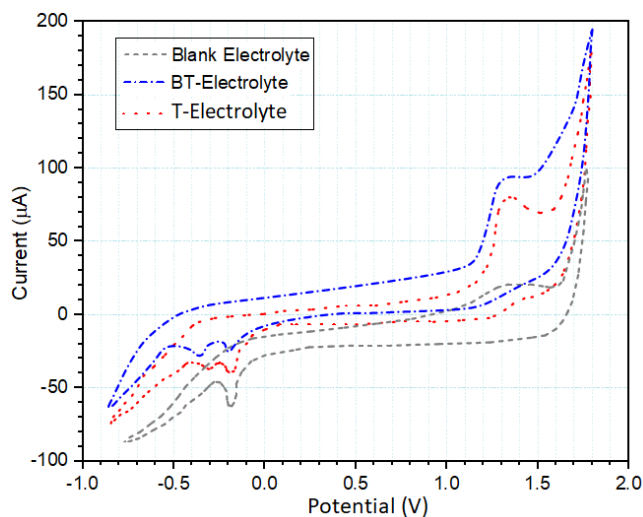


Fig. 3. XRD pattern of MoS<sub>2</sub> nanoparticles.



**Fig. 4.** Cyclic voltammogram of MoS<sub>2</sub> in a solution containing thiophene and benzothiophene (2000 mg/l) in 1.0 M H<sub>2</sub>SO<sub>4</sub> compared to that of a blank electrolyte.

Hence, the peak emerged in the presence of thiophene (T-electrolyte), and the benzothiophene (BT-electrolyte) refers to the reduction of thiophene and benzothiophene at  $-0.30$  V and  $-0.35$  V, respectively. So, a little more negative potential of BT rather than T is related to the more refractory nature of the BT compound, and consequently a more difficult reduction. Furthermore, raising the intensity of the oxidation peak on T and BT containing electrolyte at about  $1.30$  V is ascribed to the oxidation of thiophene and benzothiophene. The linear sweep voltammetry of the MoS<sub>2</sub> in the blank electrolyte and the T and/or BT containing electrolyte were compared to that of the Pt electrode in the blank electrolyte to confirm the same reduction peak (adsorption of H<sup>+</sup> on electrocatalyst) of around  $-0.20$  V. The same reduction peak (adsorption of H<sup>+</sup> on electrocatalyst) of around  $-0.20$  V for all the voltammograms was due to the adsorption of H<sup>+</sup> on this electrocatalyst, as depicted in the inset graph of Figure 5. The higher the intensity of the peak, the more the adsorption of H<sup>+</sup> occurred. Hence, the MoS<sub>2</sub> with a higher peak intensity adsorbed more H<sup>+</sup> than Pt owing to its nanosized particles and larger surface area. Also, diminishing the height of the peaks related to the MoS<sub>2</sub> in the T and BT containing electrolyte in respect to that of a blank electrolyte demonstrated that the presence of thiophenic compounds inhibited the adsorption of H<sup>+</sup>. In other words, the adsorption of H<sup>+</sup> and the thiophenic compounds on the eMoS<sub>2</sub> occurred parallelly. Furthermore, the introduction of BT and T into the electrolyte shifted the onset potential of the hydrogen evolution (HER) from  $-0.30$  V for the blank electrolyte to  $-0.40$  V and  $-0.45$  V for the T and BT containing electrolyte, respectively. This issue confirmed the increase of the HER overpotential in the presence of thiophenic compounds. The onset potential of Pt (i.e.,  $-0.25$  V) as the lowest HER overpotential electrode

was calculated from its LSV diagram to compare with the onset potential of MoS<sub>2</sub>.

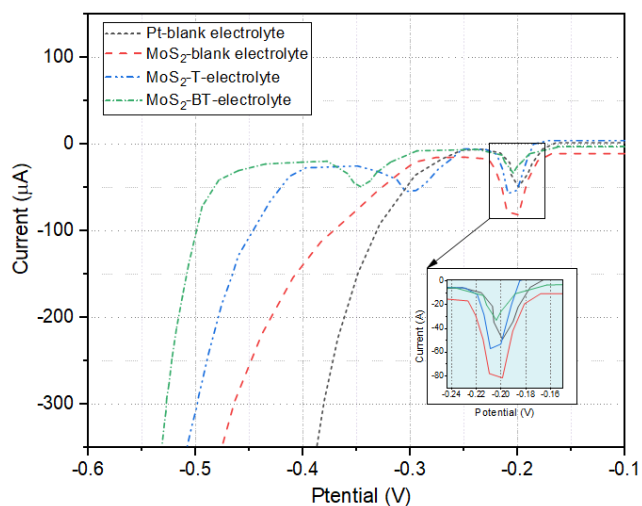


**Fig. 5.** Linear sweep voltammetry of MoS<sub>2</sub> in the thiophene and benzothiophene containing electrolyte and in the blank electrolyte and of platinum electrode in the blank electrolyte.

The apparent surface area of the MoS<sub>2</sub> ( $S_{app}$ ) electrocatalyst coated on glassy carbon was  $0.03$  cm<sup>2</sup> while the effective surface area ( $S_{eff}$ ) was measured as  $1.46$  m<sup>2</sup>, which led to a  $S_{app}/S_{eff}$  of  $46.5$ . This large surface ratio indicated that the nanosized MoS<sub>2</sub> had an electrochemical surface area of  $4.67$  cm<sup>2</sup>/g. Figure 6 depicts the Nyquist plot of MEA containing T-MoS<sub>2</sub>-Nafion and/or PEEK and Bt-MoS<sub>2</sub>-Nafion systems. Regarding the equivalent circuit of this plot, the intersection of each diagram with the  $Im(Z)$  axis at zero reveals the high resistance of the solution  $R_1$ , which can be read from the  $Re(Z)$  axis. The inverse of  $R_1$  indicates the ionic conductivity of the electrolyte. In this context, the electrolyte containing benzothiophene has a slightly higher resistant ( $0.423$  ohms) or lower conductivity than that of the electrolyte-containing thiophene ( $0.356$  ohms). This difference expresses that the more refractory sulfur compounds lead to the lower conductivity of the electrolyte due to increasing the aromaticity of refractory compounds. In Table 1, all the components of the equivalent circuit that disclose the electrochemical phenomena of the reduction process are listed. The  $Q$  (capacitive element) and  $R_2$  (resistance of electrocatalyst-membrane) are assigned to the hydrogenation and/or hydrogenolysis reaction. The  $C_d$  (double layer capacitance of carbon paper-solution) and  $R_3$  (surface impedance) are related to the desulfurization reaction. Thus, the higher  $Q$  and  $R_2$  values of T-MoS<sub>2</sub>-SPEEK represent the higher rate of HER in comparison to that of T-MoS<sub>2</sub>-Nafion. Also, the lower  $C_d$  and  $R_3$  value of T-MoS<sub>2</sub>-SPEEK than that of T-MoS<sub>2</sub>-Nafion demonstrate the weaker adsorption-diffusion of thiophene to the electrocatalyst-membrane interface and consequently results in the lower performance of the desulfurization efficiency of T-MoS<sub>2</sub>-SPEEK. Also, all the other parameters of the BT-MoS<sub>2</sub>-Nafion

system derived from the equivalent circuit prove the difficult reduction of BT. The proton conductivity of SPEEK and Nafion can determine the ion transport properties in the proton exchange membrane toward the desulfurization process. So a proton conductivity of 80.6 and 77.3 mS cm<sup>-1</sup> is in agreement with the results of the EIS experiment, which showed a lower desulfurization performance using SPEEK in comparison to Nafion.

**Table 1.** Components of equivalent circuit fitted to the Nyquist plot using T and/or BT over MoS<sub>2</sub> integrated with the Nafion or SPEEK membrane.

EIS	L	R <sub>1</sub>	Q	a	R <sub>2</sub>	C <sub>d</sub>	R <sub>3</sub>
T-MoS <sub>2</sub> -	0.356	0.24	0.08	0.58	5.43	0.05	1.21
T- MoS <sub>2</sub> -	0.382	0.26	0.09	0.59	6.74	0.06	1.74
BT-	0.436	0.42	0.18	0.75	10.3	0.17	8.93

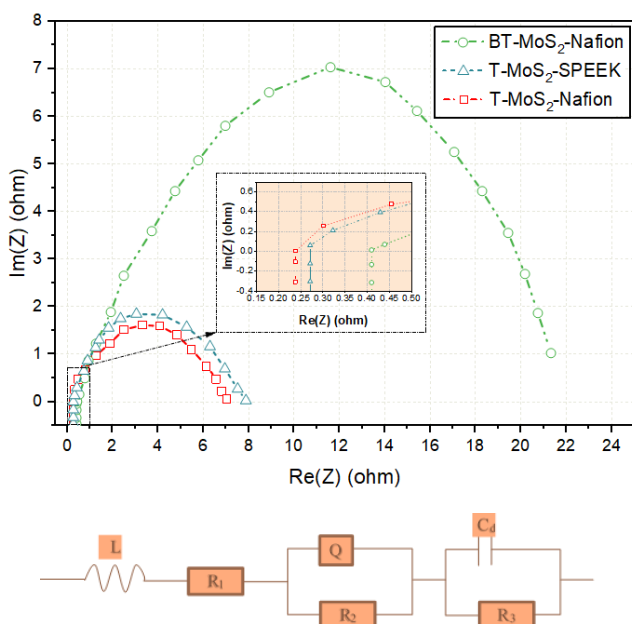


**Fig. 6.** Nyquist plot of thiophene and benzothiophene reduction at their respective reduction potential.

### 3.2. Desulfurization experiments

Regarding Figure 7, the thiophene desulfurization efficiency in an electrochemical membrane reactor using Nafion and SPEEK membranes is raised to a maximum value by increasing the current density at a constant total charge of 300 C and consequently enhancing the rate of reaction. Then, the desulfurization efficiency decreases due to the consuming of H<sup>+</sup> through its reduction to H<sub>2</sub> in parallel to the thiophene reduction. The maximum desulfurization efficiency of T on MoS<sub>2</sub> was obtained at 79.60% at 20 mA cm<sup>-2</sup> and 51.50% at 30 mA cm<sup>-2</sup> for Nafion and SPEEK, respectively. The delay in reaching the maximum value for SPEEK relative to Nafion refer to the difficult adsorption-diffusion of thiophene to the MoS<sub>2</sub>-SPEEK compared to the

MoS<sub>2</sub>-Nafion system as was demonstrated by the EIS analysis.

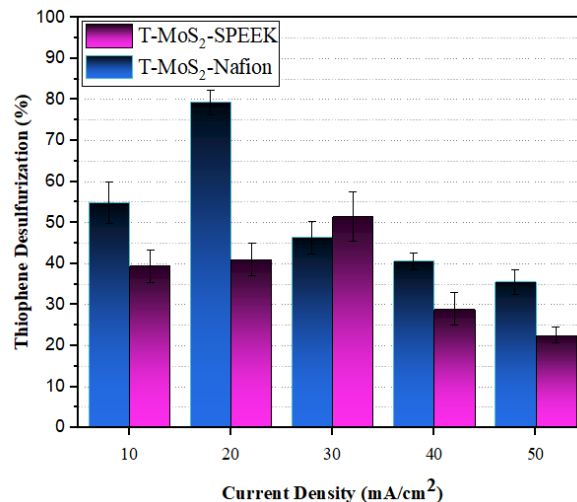


**Fig. 7.** Thiophene desulfurization efficiency of MoS<sub>2</sub> at different current density under the constant charge of 300 °C.

It was found that Nafion had a better performance toward desulfurization as an ion-exchange membrane. Thus, the benzothiophene reduction experiment was studied only using the Nafion membrane, as illustrated in Figure 8, under a different current density at a constant 400 °C. The maximum conversion of BT reached to 65.48% at 70 mA cm<sup>-2</sup>. According to Figure 8, as the current density increased from 40 to 80 mA cm<sup>-2</sup>, the hydrogenation efficiency decreased from its maximum value of 28% at 50 mA cm<sup>-2</sup>, and the desulfurization efficiency increased up to 59.08% at 70 mA cm<sup>-2</sup>. This behavior indicated that the HER would be a dominant reaction at a current density higher than 80 mA cm<sup>-2</sup>. Moreover, it can be understood that the hydrogenation reaction is prone to occur on lower current densities against desulfurization reaction, which makes it more possible at higher current densities.

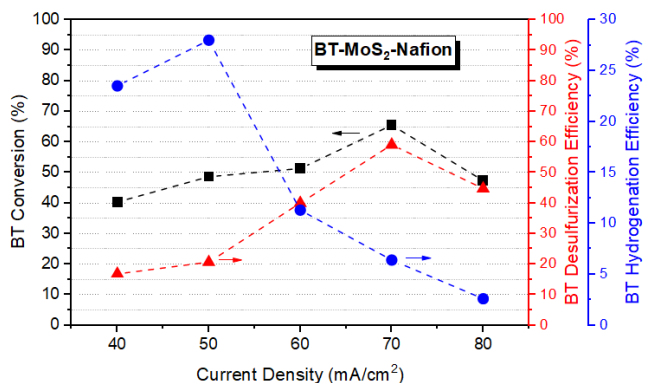


**Fig. 8.** Benzothiophene conversion, desulfurization, and hydrogenation efficiency of MoS<sub>2</sub> at different current density under the constant charge of 400 °C.

The GC-Ms analysis of T desulfurization showed no organic liquid product but had H<sub>2</sub>S as a gaseous product and unreacted thiophene. The BT desulfurization experiment

proved that H<sub>2</sub>S is the only product of the desulfurization reaction of BT and thiophene (T) according to the mechanism depicted in Figure 9. Also, figure 10 illustrates the respective GC-MS chromatogram of the initial and desulfurized model fuel containing thiophene and benzothiophene as well as some other ingredients (i.e., some hydrocarbons).

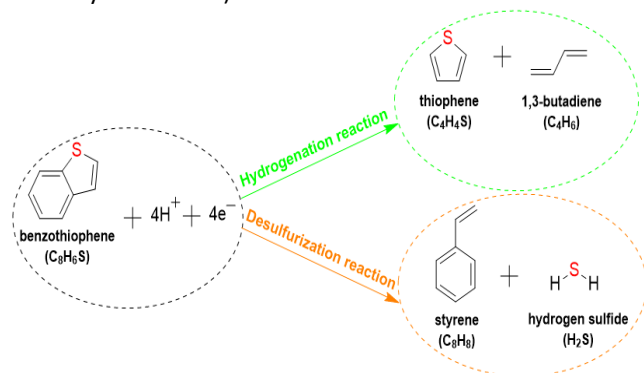


**Fig. 9.** Benzothiophene reduction mechanism using the MoS<sub>2</sub> electrocatalyst.

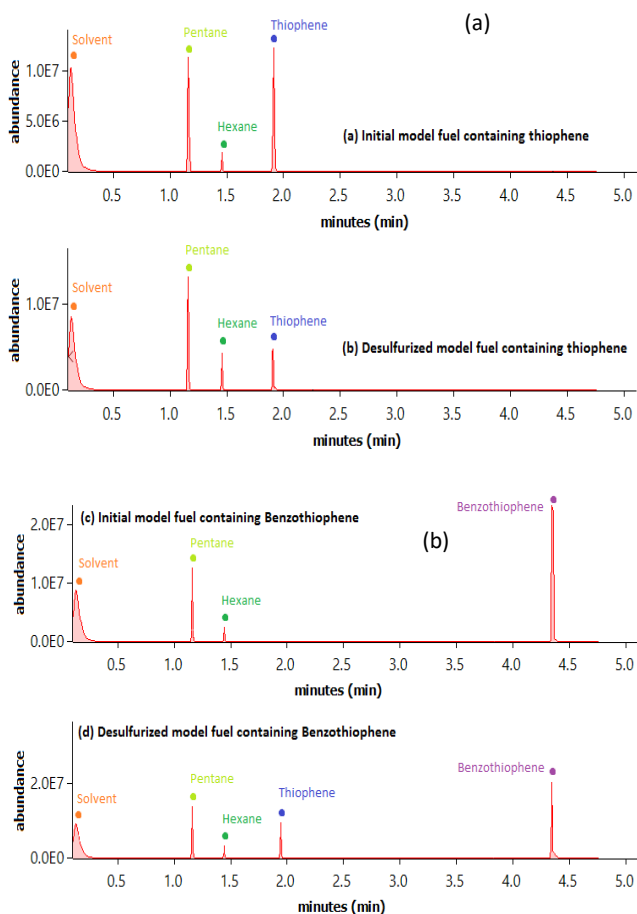


**Fig. 10.** GC-MS of model fuel containing (a) thiophene and (b) benzothiophene.

The thiophene formation during the hydrogenation pathway in the BT reduction experiment reveals that the benzene ring is more likely to react with the H<sup>+</sup> instead of

the thiophene ring in the benzothiophene at a lower current density. According to Figure 11, the yield of H<sub>2</sub>S increases from 41.69% up to 94.50% as the current density increases while the maximum yield of thiophene occurs at 40 mA cm<sup>-2</sup>, which is 58.31% and decreases to 5.49% at 80 mA cm<sup>-2</sup>. These findings are in accordance with hydrogenation and desulfurization efficiency trends. Although desulfurization efficiency increases at a higher current density, the current efficiency decreases due to increasing the rate of HER as an undesirable reaction.

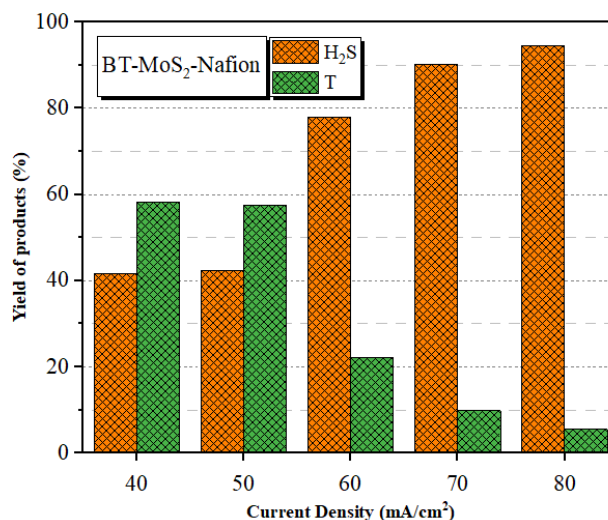


**Fig. 11.** The yield of products during benzothiophene reduction using MoS<sub>2</sub> at different current density under the constant charge of 400 °C.

#### 4. Conclusions

The viability of the electroreduction of thiophenic compounds through the electrochemical membrane reactor was demonstrated over a MoS<sub>2</sub> electrocatalyst integrated with a proton exchange membrane such as Nafion and SPEEK. The results of this study have shown that direct desulfurization is the only pathway to thiophene reduction, while hydrogenation is a rival reaction along with benzothiophene direct desulfurization. This issue implies that the probability of hydrogenation of unsaturated bonds increases with the number of the benzene rings in thiophenic compounds. Also, the current density can control the reaction pathway so that on a lower current density, the BT hydrogenation is dominant and approaches to 28% at 50 mA cm<sup>-2</sup>, while desulfurization is the main pathway on higher current densities and reaches to 59.08% at 70 mA cm<sup>-2</sup>. The maximum desulfurization efficiency of T-MoS<sub>2</sub>-Nafion (i.e., 79.6% at 20 mA cm<sup>-2</sup>) proves the higher performance of this system towards desulfurization in comparison with T-MoS<sub>2</sub>-SPEEK (and 51.5% at 30 mA cm<sup>-2</sup>). The higher constant charge that is needed to reach an acceptable desulfurization efficiency of benzothiophene relative to those required in the thiophene reduction process indicates the higher resistance in the

desulfurization of more refractory sulfur compounds. Finally, MoS<sub>2</sub> can be a promising electrocatalyst towards the desulfurization of thiophenic compounds individually or mixed with a platinum electrocatalyst due to its significant desulfurization efficiency and lower cost compared to Pt (as the most active electrocatalyst toward desulfurization of the thiophenic compound).

### Acknowledgment

The authors gratefully acknowledge the financial support of the present work (project no. 95849150) by the Iran National Science Foundation (INSF).

### References

- [1] Lam, V., Li, G., Song, C., Chen, J., Fairbridge, C., Hui, R., Zhang, J. (2012). A review of electrochemical desulfurization technologies for fossil fuels. *Fuel processing technology*, 98, 30-38.
- [2] Liu, D., Li, M., Al-Otaibi, R. L., Song, L., Li, W., Li, Q., Yan, Z. (2015). Study on the Desulfurization of High-Sulfur Crude Oil by the Electrochemical Method. *Energy and fuels*, 29(11), 6928-6934.
- [3] Babich, I. V., Moulijn, J. A. (2003). Science and technology of novel processes for deep desulfurization of oil refinery streams: a review. *Fuel*, 82(6), 607-631.
- [4] Zhong, S. T., Zhao, W., Sheng, C., Xu, W. J., Zong, Z. M., Wei, X. Y. (2011). Mechanism for removal of organic sulfur from guiding subbituminous coal by electrolysis. *Energy and fuels*, 25(8), 3687-3692.
- [5] Song, C. (2003). An overview of new approaches to deep desulfurization for ultra-clean gasoline, diesel fuel and jet fuel. *Catalysis today*, 86(1-4), 211-263.
- [6] Song, C. (2002). New approaches to deep desulfurization for ultra-clean gasoline and diesel fuels: an overview. *Preprints of papers- American chemical society, division of fuel chemistry*, 47(2), 438-444.
- [7] Di, L., Chenguang, L. (2013). Deep hydrodesulfurization of diesel fuel over diatomite-dispersed NiMoW sulfide catalyst. *China petroleum processing and petrochemical technology*, 15(4), 38-43.
- [8] Kim, T., Ali, S. A., Alhooshani, K., Park, J. I., Al-Yami, M., Yoon, S. H., Mochida, I. (2013). Analysis and deep hydrodesulfurization reactivity of Saudi Arabian gas oils. *Journal of industrial and engineering chemistry*, 19(5), 1577-1582.
- [9] Vogelaar, B. M., Steiner, P., van der Zijden, T. F., van Langeveld, A. D., Eijsbouts, S., Moulijn, J. A. (2007). Catalyst deactivation during thiophene HDS: The role of structural sulfur. *Applied catalysis A: general*, 318, 28-36.
- [10] Wang, H, Prins, R. (2008). HDS of benzothiophene and dihydrobenzothiophene over sulfided Mo/γ-Al<sub>2</sub>O<sub>3</sub>. *Applied catalysis A: general*, 350(2), 191-196.
- [11] Wang, J., Zhang, L., Sun, Y., Jiang, B., Chen, Y., Gao, X., Yang, H. (2018). Deep catalytic oxidative desulfurization of fuels by novel Lewis acidic ionic liquids. *Fuel processing technology*, 177, 81-88. 4.
- [12] Bertleff, B., Claußnitzer, J., Korth, W., Wasserscheid, P., Jess, A., Albert, J. (2017). Extraction coupled oxidative desulfurization of fuels to sulfate and water-soluble sulfur compounds using polyoxometalate catalysts and molecular oxygen. *ACS sustainable chemistry and engineering*, 5(5), 4110-4118.
- [13] Zeelani, G. G., Ashrafi, A., Dhakad, A., Gupta, G., Pal, S. L. (2016). Catalytic oxidative desulfurization of liquid fuels: a review. *International research journal of engineering and technology*, 3(5) 331-336.
- [14] Abbasov, V. M., Ibrahimov, H. C., Mukhtarova, G. S., Rustamov, M. I., Abdullayev, E. (2017). Adsorptive Desulfurization of the Gasoline Obtained from Low-Pressure Hydrocracking of the Vacuum Residue Using a Nickel/Bentonite Catalyst. *Energy and fuels*, 31(6), 5840-5843.
- [15] Ahmed, I, Jhung, S. H. (2016). Adsorptive desulfurization and denitrogenation using metal-organic frameworks. *Journal of hazardous materials*, 301, 259-276.
- [16] Ghanbarlou, H., Rowshanzamir, S., Parnian, M. J., Mehri, F. (2016). Comparison of nitrogen-doped graphene and carbon nanotubes as supporting material for iron and cobalt nanoparticle electrocatalysts toward oxygen reduction reaction in alkaline media for fuel cell applications. *International journal of hydrogen energy*, 41(33), 14665-14675.
- [17] Mehri, F., Sauter, W., Schröder, U., Rowshanzamir, S. (2019). Possibilities and constraints of the electrochemical treatment of thiophene on low and high oxidation power electrodes. *Energy and fuels*, 33(3), 1901-1909.
- [18] Baatar, B., Gan-Erdene, T., Myekhlai, M., Otgonbayar, U., Majaa, C., Turmunkh, Y., Javkhlantugs, N. (2017). Desulfurization of coal using the electrochemical technique in neutral and alkaline media. *Energy sources, part A: recovery, utilization, and environmental effects*, 39(15), 1610-1616.
- [19] Lam, V., Li, G., Song, C., Chen, J., Fairbridge, C., Hui, R., Zhang, J. (2012). A review of electrochemical desulfurization technologies for fossil fuels. *Fuel processing technology*, 98, 30-38.
- [20] Basile, A., Di Paola, L., Hai, F., Piemonte, V. (Eds.). (2015). Membrane reactors for energy applications and basic chemical production, *Woodhead Publishing*.
- [21] García-Cruz, L., Casado-Coterillo, C, Irabien, Á, Montiel, V, Iniesta, J. (2016). Performance assessment of a polymer electrolyte membrane electrochemical reactor under alkaline conditions – A case study with the electrooxidation of alcohols. *Electrochimica acta*, 206, 165-175.
- [22] Fonocho, R., Gardner, C. L., Terman, M. (2012). A study of the electrochemical hydrogenation of o-xylene in a

- PEM hydrogenation reactor. *Electrochimica acta*, 75, 171-178.
- [23] Liu, L., Liu, H., Huang, W., He, Y., Zhang, W., Wang, C., Lin, H. (2017). Mechanism and kinetics of the electrocatalytic hydrogenation of furfural to furfuryl alcohol. *Journal of electroanalytical chemistry*, 804, 248-253.
- [24] Báez, V., D'elia, L. F., Rodriguez, G., Gandica, Y. (2013). *U.S. Patent No. 8,617,477*. Washington, DC: U.S. patent and trademark office.
- [25] Greaney, M. A., Wang, K., Wang, F. C. (2009). *U.S. patent application No. 12/288,565*.
- [26] D'Elia Camacho, L. F., Puentes, Z., Calderón, J., Lucena, E., Moncada, J., Saavedra, K. (2011). Assisted electrochemical hydroconversion of heterocompounds present in fuel and oil using active hydrogen passing through a Pd membrane. *Petroleum science and technology*, 29(5), 529-534.
- [27] Sedighi, S., Gardner, C. L. (2010). A kinetic study of the electrochemical hydrogenation of ethylene. *Electrochimica acta*, 55(5), 1701-1708.
- [28] Huang, H., Yu, Y., Chung, K. H. (2012). Seasonal storage of electricity by hydrogen in benzene–water system. *International journal of hydrogen energy*, 37(17), 12798-12804.
- [29] Nagarale, R. K., Gohil, G. S., Shahi, V. K. (2006). Recent developments on ion-exchange membranes and electro-membrane processes. *Advances in colloid and interface science*, 119(2-3), 97-130.
- [30] Swier, S., Chun, Y. S., Gasa, J., Shaw, M. T., Weiss, R. A. (2005). Sulfonated poly (ether ketone ketone) ionomers as proton exchange membranes. *Polymer engineering and science*, 45(8), 1081-1091.
- [31] Mikami, T., Miyatake, K., Watanabe, M. (2010). Poly (arylene ether) s containing superacid groups as proton exchange membranes. *ACS applied materials and interfaces*, 2(6), 1714-1721.
- [32] Liu, Y. L. (2012). Developments of highly proton-conductive sulfonated polymers for proton exchange membrane fuel cells. *Polymer chemistry*, 3(6), 1373-1383.
- [33] Basile, A. (Ed.). (2013). *Handbook of membrane reactors: fundamental materials science, design and optimisation*. Elsevier.
- [34] Behrouzifar, A., Rowshanzamir, S., Alipoor, Z., Bazmi, M. (2016). Application of a square wave potentiometry technique for electroreductive sulfur removal from a thiophenic model fuel. *International journal of environmental science and technology*, 13(12), 2883-2892.
- [35] Alipoor, Z., Behrouzifar, A., Rowshanzamir, S., Bazmi, M. (2015). Electrooxidative desulfurization of a thiophene-containing model fuel using a square wave potentiometry technique. *Energy and fuels*, 29(5), 3292-3301.
- [36] Zhao, W, Zhu, H., Zong, Z. M, Xia, J. H, Wei, X. Y. (2005). Electrochemical reduction of pyrite in aqueous NaCl solution. *Fuel*, 84(2-3), 235-238.
- [37] Shu, C., Sun, T., Jia, J., Lou, Z. (2013). Mild process for reductive desulfurization of diesel fuel using sodium borohydride in situ generated via sodium metaborate electroreduction. *Industrial and engineering chemistry research*, 52(23), 7660-7667.
- [38] Huang, H., Yuan, P., Yu, Y., Chung, K. H. (2017). Electrochemical hydrogenation of organic sulfides. *International journal of hydrogen energy*, 42(29), 18203-18208.
- [39] Infantes-Molina, A., Romero-Pérez, A., Eliche-Quesada, D., Mérida-Robles, J., Jiménez-López, A., Rodríguez-Castellón, E. (2012). Transition metal sulfide catalysts for petroleum upgrading–Hydrodesulfurization Reactions. In *hydrogenation*. In tech open.
- [40] Tye, C. T., Smith, K. J. (2006). Catalytic activity of exfoliated MoS<sub>2</sub> in hydrodesulfurization, hydrodenitrogenation and hydrogenation reactions. *Topics in catalysis*, 37(2-4), 129-135.
- [41] Kim, H.K. *et al.* (2016) Preparation of CoMo/Al<sub>2</sub>O<sub>3</sub>, CoMo/CeO<sub>2</sub>, CoMo/TiO<sub>2</sub> catalysts using ultrasonic spray pyrolysis for the hydro-desulfurization of 4, 6-dimethyldibenzothiophene for fuel cell applications. *International journal hydrogen energy* 41, 18846–18857.
- [42] Ahn, H.S. and Bard, A.J. (2016) Electrochemical surface interrogation of a MoS<sub>2</sub> Hydrogen-eolving catalyst: In situ determination of the surface hydride coverage and the Hydrogen evolution Kinetics. *Journal of physical chemistry. Letter.* 7, 2748–2752.
- [43] Stephenson, T. *et al.* (2014) Lithium ion battery applications of molybdenum disulfide (MoS<sub>2</sub>) nanocomposites. *Energy and environmental science.* 7, 209–231.
- [44] Gao, Y. P., Huang, K. J., Wu, X., Hou, Z. Q., Liu, Y. Y. (2018). MoS<sub>2</sub> nanosheets assembling three-dimensional nanospheres for enhanced-performance supercapacitor. *Journal of alloys and compounds*, 741, 174-181.
- [45] Domínguez-Meister, S., Rojas, T. C., Brizuela, M., Sánchez-López, J. C. (2017). Solid lubricant behavior of MoS<sub>2</sub> and WSe<sub>2</sub>-based nanocomposite coatings. *Science and technology of advanced materials*, 18(1), 122-133.
- [46] Zhang, X.H. , Wang, C. , Xue, M.Q. , Lin, B.C., Ye, X., Lei, W.N. (2016) Hydrothermal synthesis and charecterization of ultrathin MoS<sub>2</sub> nanoshits. *Chalcogenide letters.* 13, 27–34.
- [47] Jin, Q., Chen, B., Ren, Z., Liang, X., Liu, N., Mei, D. (2018) A theoretical study on reaction mechanisms and kinetics of thiophene hydrodesulfurization over MoS<sub>2</sub> catalysts. *Cataysis. today* 312, 158–167.

- [48] Farag, H., El-Hendawy, A.A., Sakanishi, K., Kishida, M., Mochida, I. (2009) Catalytic activity of synthesized nanosized molybdenum disulfide for the hydrodesulfurization of dibenzothiophene: Effect of H<sub>2</sub>S partial pressure. *Applied catalysis B: Environmental journal*. 91, 189–197.
- [50] Karthika, A., Raja, R., Karuppasamy, P., Suganthi, A., Rajarajan, M. (2019) Electrochemical behaviour and voltammetric determination of mercury (II) ion in cupric oxide/poly vinyl alcohol nanocomposite modified glassy carbon electrode. *Microchemical journal*. 145, 737–744.
- [51] McCrum, I.T., Janik, M.J. (2017) Deconvoluting Cyclic Voltammograms To Accurately Calculate Pt Electrochemically Active Surface Area. *Journal of physical Chemistry. C* 121, 6237–6245.
- [52] Trasatti, S., Petrii, O.A. (1992) Real surface area measurements in electrochemistry. *Journal of electroanalytical chemistry*. 327, 353–376.